


## Article

# Cerebral Cavernous Malformation 1 Determines YAP/TAZ Signaling-Dependent Metastatic Hallmarks of Prostate Cancer Cells

Sangryong Park <sup>1,†</sup>, Ho-Young Lee <sup>1,2,†</sup>, Jayoung Kim <sup>3,†</sup>, Hansol Park <sup>4</sup>, Young Seok Ju <sup>4</sup>, Eung-Gook Kim <sup>5</sup> and Jaehong Kim <sup>1,2,\*</sup> 

- <sup>1</sup> Department of Biochemistry, College of Medicine, Gachon University, Incheon 21999, Korea; rustlove@naver.com (S.P.); yiyounjgk@gmail.com (H.-Y.L.)
- <sup>2</sup> Department of Health Sciences and Technology, Gachon Advanced Institute for Health Science and Technology, Gachon University, Incheon 21999, Korea
- <sup>3</sup> Division of Cancer Biology and Therapeutics, Departments of Surgery & Biomedical Sciences, Samuel Oschin Comprehensive Cancer Institute, Cedars-Sinai Medical Center, Los Angeles, CA 90048, USA; Jayoung.Kim@csmc.edu
- <sup>4</sup> Graduate School of Medical Science and Engineering, Korea Advanced Institute of Science and Technology, Daejeon 34141, Korea; hs0530@kaist.ac.kr (H.P.); ysj@kaist.ac.kr (Y.S.J.)
- <sup>5</sup> Department of Biochemistry, Chungbuk National University College of Medicine, Cheongju 28644, Korea; egkim@chungbuk.ac.kr
- \* Correspondence: geretics@gachon.ac.kr; Tel.: +82-32-899-6441
- † These authors contributed equally.



**Citation:** Park, S.; Lee, H.-Y.; Kim, J.; Park, H.; Ju, Y.S.; Kim, E.-G.; Kim, J. Cerebral Cavernous Malformation 1 Determines YAP/TAZ Signaling-Dependent Metastatic Hallmarks of Prostate Cancer Cells. *Cancers* **2021**, *13*, 1125. <https://doi.org/10.3390/cancers13051125>

Academic Editor:  
Francisco Wandosell

Received: 23 December 2020  
Accepted: 2 March 2021  
Published: 5 March 2021

**Publisher's Note:** MDPI stays neutral with regard to jurisdictional claims in published maps and institutional affiliations.



**Copyright:** © 2021 by the authors. Licensee MDPI, Basel, Switzerland. This article is an open access article distributed under the terms and conditions of the Creative Commons Attribution (CC BY) license (<https://creativecommons.org/licenses/by/4.0/>).

**Simple Summary:** Our analysis of cerebral cavernous malformation 1 (CCM1) expression and function reveals a candidate predictive biomarker for prostate cancer metastasis and provides evidence that CCM1 abnormality can be pathogenic in prostate cancer. In particular, the CCM1 regulation of metastasis appears as a common molecular event in metastatic prostate cancer cells arising from disparate genetic backgrounds.

**Abstract:** Enhanced Yes-associated protein (YAP)/transcriptional co-activator with PDZ-binding motif (TAZ) signaling is correlated with the extraprostatic extension of prostate cancer. However, the mechanism by which YAP/TAZ signaling becomes hyperactive and drives prostate cancer progression is currently unclear. In this study, we revealed that higher expression of CCM1, which is uniquely found in advanced prostate cancer, is inversely correlated with metastasis-free and overall survival in patients with prostate cancer. We also demonstrated that CCM1 induces the metastasis of multiple types of prostate cancer cells by regulating YAP/TAZ signaling. Mechanistically, CCM1, a gene mutated in cerebral cavernous malformation, suppresses DDX5, which regulates the suppression of YAP/TAZ signaling, indicating that CCM1 and DDX5 are novel upstream regulators of YAP/TAZ signaling. Our findings highlight the importance of CCM1-DDX5-YAP/TAZ signaling in the metastasis of prostate cancer cells.

**Keywords:** cerebral cavernous malformation; prostate cancer; metastasis; DDX5; YAP/TAZ signaling

## 1. Introduction

Prostate cancer (PCa) is a clinically heterogeneous disease with marked variability in patient outcomes [1–3]. Importantly, PCa is also the second most common cause of male cancer death worldwide. Indeed, PCa is a disease entity for which no effective therapies exist once it progresses to metastatic castration-resistant PCa (mCRPC), and clinically advanced PCa is responsible for more than 250,000 deaths worldwide annually [4,5].

Advancements in therapeutic strategies for PCa have led to a surge in the incidence of metastasis, indicating the importance of preventing these detrimental metastatic

events [6,7]. Diverse sets of cancer hallmarks associated with aberrant functioning of the androgen receptor (AR), which is induced by androgen deprivation therapy (ADT), are the key driving forces behind the uncontrollable growth and metastasis of PCa and its transition into mCRPC [8–10]. However, the clinically heterogeneous, multifocal nature of PCa along with the late appearance of castration resistance (CR) and the resultant uncontrollable bone metastasis makes the disease frustratingly complex to investigate and treat [10,11]. Therefore, identifying the central molecular changes caused by current ADT-based therapeutic interventions, ultimately leading to the acquisition of uncontrollable metastasis, is critical for gaining important insights into key unmet needs, namely the improvement of diagnostic biomarkers and therapeutic interventions for mCRPC.

Yes-associated protein (YAP) and transcriptional co-activator with PDZ-binding motif (TAZ) signaling pathways have emerged as important drivers of the development, growth, and metastasis of human malignancies including PCa, and accumulating evidence has illustrated that YAP/TAZ signaling is correlated with the metastasis of PCa [12,13]. YAP or TAZ is a transcriptional co-activator that interacts with the transcription factor TEAD. Promoter regions of YAP/TAZ target genes have TEAD binding sites, and the interaction of YAP or TAZ with a member of the TEAD family of transcription factors increases TEAD transcriptional activity. Increased expression of YAP or TAZ or their nuclear localization is observed significantly more frequently in mCRPC than in primary PCa, and disruption of YAP/TAZ or AR signaling suppresses the castration-resistant growth, motility, and invasion of PCa cells [12–15]. Elevated YAP/TAZ signaling is also a positive regulator of AR signaling, and it is responsible for CR and metastasis, indicating the significance of YAP/TAZ signaling in PCa progression [12,15]. However, the mechanism by which YAP/TAZ signaling becomes hyperactive and drives PCa progression is currently unclear.

In the present study, we sought to clarify the novel cerebral cavernous malformation 1 (CCM1)-mediated regulatory mechanism of YAP/TAZ signaling in PCa progression using multiple PCa cell types. The functional disturbances from mutations in one of three genes: CCM1 (Krit1; Krev interaction trapped 1), CCM2 (MGC4607, Malcavernin) and CCM3 (PDCD10) are known to be responsible for CCMs. Typical histological presentations of CCMs are vascular leakage at the brain capillary level, disruption of the blood-brain barrier (BBB), and single or multiple lumen formation in the central nervous system (CNS) [16]. CCM1 and CCM2 proteins participate in common signaling pathways [17] and the strong interaction between CCM1 and CCM2 is important for the regulation of CCM signaling in endothelial cells [18,19]. CCM3 appears to act in different signaling pathways [17,20–22]. From our preliminary molecular cohort studies, CCM1 and DDX5 were among the genes that we found the expression levels were changed exclusively in mCRPC patients. Since we previously identified the interaction between CCM1 and DDX5 from an unreported proteomics study, this finding prompted us to investigate the detailed mechanism of CCM1 first in regulating metastatic potencies of PCa cells. Notably, most studies on the CCM gene have been conducted in the field of vascular biology, and there is limited understanding regarding its function in cancer biology [23,24].

## 2. Results

### 2.1. Higher Expression of *Ccm1* at the *Mcrpc* Stage and Its Association with Poor Prognosis of Patients with PCa

We analyzed changes in the expression of CCM1 gene during PCa progression using data from multiple human PCa cohort studies. From the GDS2545 and GDS2547 datasets [25], we observed that CCM1 expression was remarkably increased in mCRPC samples (Figure 1A–B). Next, we applied a larger dataset from the PCa transcriptome atlas (PCTA), which we recently built using integrated bioinformatics analysis methods [26]. From the PCTA, we also observed that CCM1 levels were dramatically increased only in samples from patients with mCRPC compared with those in primary prostate tissue and other stages of PCa (Figure 1C–D and Figure S1A–C). The stem plots with different colors in Figure 1C illustrate that average CCM1 level was uniquely increased in mCRPC. The waterfall plot in Figure 1D displays normalized CCM1 gene expression for individual

samples. We further examined the expression of CCM2 and CCM3, other members of the CCM family. Contrary to the findings for CCM1, we observed no meaningful increases of CCM2 or CCM3 expression during PCa progression (Figure 1E and Figure S1D–F). The specific increase of CCM1 expression in the advanced stage of PCa suggests its potential as an index of poor prognosis for patients with PCa. We therefore analyzed the associations of CCM1 expression with overall survival (OS) in the Swedish Watchful Waiting cohort [27] and with metastasis-free survival in the Johns Hopkins cohort [28] (Figure 1F). We observed inverse correlations of CCM1 expression with OS and metastasis-free survival. Our analysis illustrated that increased CCM1 expression was significantly associated with poor prognosis for patients with PCa.

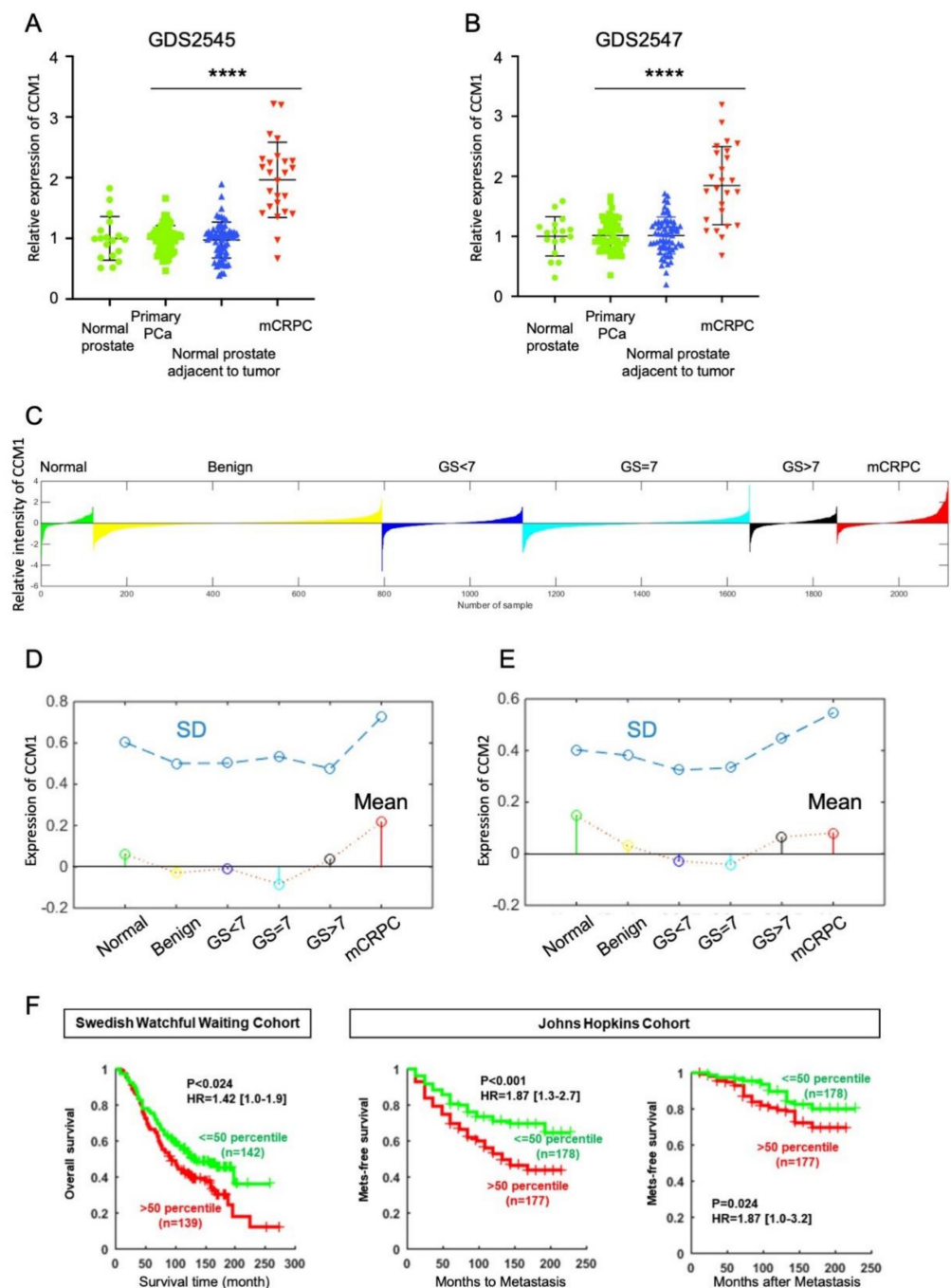


**Figure 1.** CCM1 levels are increased exclusively in metastatic castration-resistant prostate cancer (mCRPC) samples. (A,B) Relative CCM1 mRNA levels in normal prostate tissue ( $n = 17$ ), normal

prostate tissue adjacent to the tumor ( $n = 58$ ), and primary ( $n = 64$ ) and mCRPC ( $n = 25$ ) tumors. Data were retrieved from accession numbers GDS2545 (A) and GDS2547 (B) of the Gene Expression Omnibus database. Data are presented as the mean  $\pm$  SD. t-test results between mCRPC and primary PCa: (\*\*\*\*:  $p < 0.0001$ ). (C) This waterfall plot displays normalized CCM1 gene expression levels in individual samples from the prostate cancer transcriptome atlas (PCTA) cohort ( $n = 2115$ ), which includes normal ( $n = 121$ ); benign (benign prostatic hyperplasia,  $n = 673$ ); primary prostate cancer (PCa) with Gleason Sum (GS)  $< 7$  ( $n = 328$ ), GS = 7 ( $n = 530$ ), or GS  $> 7$  ( $n = 203$ ); and mCRPC samples ( $n = 260$ ). The x-axis presents samples, and the y-axis presents normalized gene expression (log<sub>2</sub> scale). The Wilcoxon rank sum test results between subsets (mCRPC vs. primary PCa): Fold change = 0.256,  $p < 0.001$ . (D) The stem plots with different colors show the mean expression levels of CCM1 in each disease state from the PCTA cohort. The x-axis presents the disease state, and the y-axis presents normalized gene expression. The dot plot above the stem plot represents the variance (SD) of gene expression values of the samples from the same disease state. (E) The stem plots with different colors show the mean expression levels of CCM2 in each disease state. (F) To assess the association of CCM1 gene expression with overall or metastasis-free survival, clinical information was extracted from the Swedish Watchful Waiting Cohort (left) and Johns Hopkins Cohort (right two panels). Patients in each cohort were subdivided into “low” ( $< 50$ th percentile) or “high” ( $\geq 50$ th percentile) CCM1 expression groups. Kaplan–Meier curves for overall and metastasis-free survival were drawn for each category, and Cox proportional hazard regression analysis was performed for statistical comparisons of survival rates between the low and high expression groups.

## 2.2. CCM1 Induces Metastatic Hallmarks of PCa Cells

Different PCa cell models possess distinct tumorigenic subpopulations that both commonly and uniquely express important signaling pathways [29]. Considering the potential regulatory function of CCM1 in metastasis, we examined its involvement in metastasis-related features in multiple types of metastatic PCa cells. We generated a series of shCCM1 cell lines (PC3, DU145, LNCaP, C4-2, C4-2B, and CWR22r) in which CCM1 expression was stably suppressed using RNAi and, just prior to each experiments, always validated that more than 70% of CCM1 was suppressed in each shCCM1 cells relative to scramble cells. We investigated changes in migration and invasion following CCM1 suppression using wound-healing assay and Transwell migration and invasion assays. Both PC3 and DU145 shCCM1 cells exhibited delayed wound closure, indicating that cell migration was hampered (Figure 2A). Our Transwell assays using PC3, DU145, C4-2, and CWR22r shCCM1 cells revealed that CCM1 suppression reduced both migration and invasion in multiple metastatic PCa cell lines (Figure 2B and Figure S2A–C). Cadherin switching, which is induced via the repression of E-cadherin and upregulation of N-cadherin, is a phenotype that represents a major hallmark of the metastatic process in most types of epithelial cancer [30,31]. PC3 shCCM1 cells grown in a 3D hanging drop culture system or 2D culture plate system uniformly exhibited E-cadherin upregulation and N-cadherin downregulation (Figure 2C and Figure 4C,E), indicating that CCM1 upregulation can induce cadherin switching. Because DU145 cells do not express N-cadherin, PC3 cells were used for the cadherin switching analysis in this study [32]. SLUG, SNAIL, and TWIST are representative transcription factors responsible for epithelial-mesenchymal transition (EMT) gene signatures including cadherin switching [33,34]. qPCR analysis indicated that both SLUG and TWIST expression was reduced in our shCCM1 cells (Figure 2D), whereas SNAIL expression was not affected (Figure S2E). All primers for qPCR are described in Table S1. Our soft agar assay revealed that CCM1 is necessary for the anchorage-independent survival of PCa cells (Figure 2E and Figure S2D). Suppression of CCM1 prominently reduced the survival of PC3 and DU145 cells in clonogenic survival assays (Figure 2F). From proliferation assay and flow cytometry analysis, we found that suppression of CCM1 did not affect proliferation rates or cell cycle progression (Figure S2F). We conclude that CCM1 upregulates the migration (motility), invasion, and survival of PCa cells.

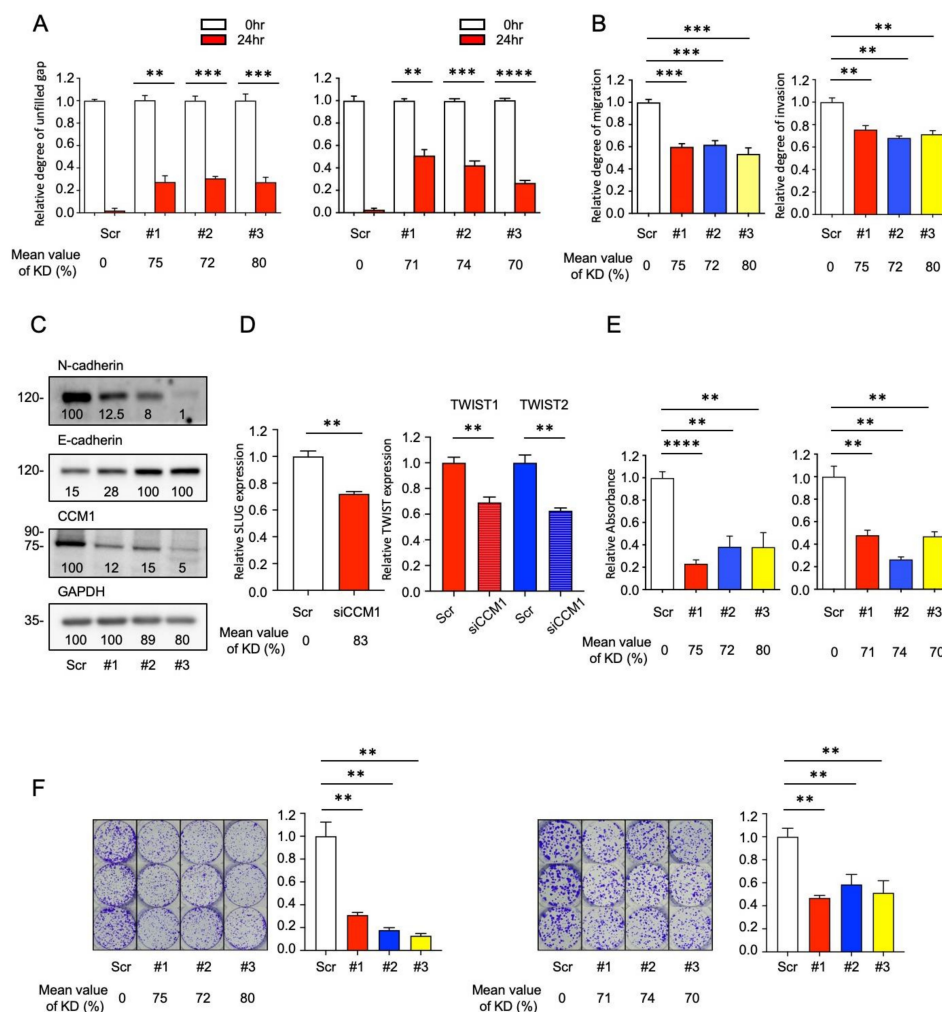


**Figure 2.** Suppression of CCM1 downregulates metastatic hallmarks in prostate cancer cells in vitro. (A) Scratch wounds were created in fully confluent PC3 (left) and DU145 shCCM1 cells (right), and unfilled gaps were measured after 24 h. The data are presented as the mean  $\pm$  SEM of the unclosed length expressed as a ratio to that at 0 h. Functional assays of Figure 2A can be found in Supplementary File 2. (B) PC3 shCCM1 cells were plated on Transwell membranes coated without or with Matrigel for migration (left) and invasion assays (right), respectively, incubated for up to 72 h, and stained. Data are presented as the mean  $\pm$  SEM of a ratio to that in scramble (Scr) control level. Functional assays of Figure 2B can be found in Supplementary File 2. (C) PC3 shCCM1 cells were grown in 3D hanging drop culture for 3 days, and protein extracts were analyzed for changes in N-cadherin and E-cadherin expression via immunoblotting. Band intensities are shown in each panel. Uncropped Blots of Figure 2C can be found Supplementary File 2. (D) SLUG expression in PC3 (left) and TWIST1 and TWIST2 expression (right) were analyzed by qPCR in CCM1-suppressed PC3 and C4-2 cells, respectively. Data are presented as the mean  $\pm$  SEM of a ratio to that in the scramble (Scr) control level. (E) PC3 (left) and DU145 (right) shCCM1 cells were grown in soft agar for 7 days, and lysates were analyzed using a microplate reader to measure anchorage-independent survival. The data are presented as the mean  $\pm$  SEM of absorbance expressed as a ratio to that in Scr control. (F) PC3 (left) and DU145 shCCM1 cells (right) were plated in each well of a six-well plates, grown for 10 days, and stained with crystal violet for clonogenic survival assays. Representative images were presented from three independent experiments, and graphs were generated from three independent experiments. Average levels of CCM1 knockdown were measured from qPCR analysis and presented below each panel. t-test results (\*\*\*\*:  $p < 0.0001$ , \*\*\*:  $p < 0.001$ , \*\*:  $p < 0.01$ ).

### 2.3. CCM1 Regulates YAP/TAZ Signaling

As stated previously, accumulated evidence indicates that YAP/TAZ signaling is correlated with PCa metastasis. We thus investigated whether CCM1 upregulates YAP/TAZ signaling. As expected, the overexpression of CCM1 increased the activity of the TEAD



reporter (8XGTIIC luciferase) in PC3 and LNCaP cells (Figure S3A). Because CCM1 was not overexpressed robustly with plasmid transfection and our attempt to overexpress CCM1 modestly increased TEAD reporter activity in PC3, LNCaP (Figure S3A), and C4-2 cells, we focused on CCM1 suppression in further studies. We also characterized the effect of AR signaling on CCM1 function using dihydrotestosterone (DHT) stimulation. Aberrant AR signaling is associated with the progression of PCa. CCM1 silencing decreased TEAD reporter activity in androgen responsive LNCaP and C4-2 cells regardless of DHT stimulation (Figure 3A,B). The suppression of CCM1 also reduced TEAD reporter activity in androgen nonresponsive DU145 cells (Figure 3C), indicating that CCM1-mediated regulation of YAP/TAZ signaling was functional in multiple types of PCa cells. We also sorted PC3 cells stably expressing ectopic AR into AR high and AR low clones (Figure S3B). Although WT PC3 cells do not respond to DHT stimulation, they retain multiple AR co-activators and repressors, and the introduction of ectopic AR restores androgen responsiveness in PC3 cells (Figure S3C), as reported previously [35]. The suppression of CCM1 also reduced TEAD reporter activity in AR low and AR high PC3 cells regardless of DHT stimulation (Figure S3D). Using qPCR analysis, we also confirmed that the expression of representative YAP/TAZ target genes such as *Ankrd1*, *Birc5*, *Ctgf*, and *Cyr61* was downregulated by the RNAi-mediated silencing of CCM1 (Figure 3D). Suppression of CCM1 by siRNA transfection was effective in multiple types of PCa cells (Figure 3E). Our siRNA based CCM1 knockdown showed 70~90% suppression of CCM1 relative to the scramble control. Our data indicate that suppression of CCM1 downregulates YAP/TAZ activity regardless of androgen responsiveness in PCa cells.

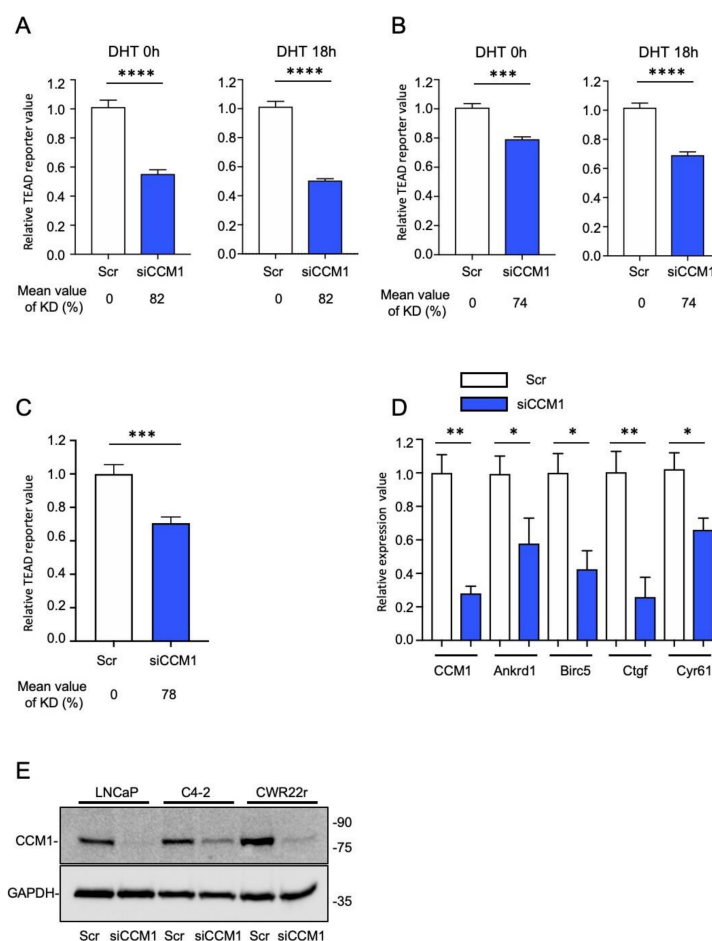


**Figure 3.** CCM1 upregulates YAP/TAZ signaling. (A) LNCaP and (B) C4-2 cells were co-transfected with CCM1 siRNA and TEAD reporter plasmids. Cells were grown in charcoal-stripped FBS-supplemented

medium and stimulated with or without 1  $\mu$ M DHT for 18 h, as indicated. Reporter activities are shown as relative to that in scramble (Scr) control cells. (C) CCM1 was RNAi-silenced in DU145 cells grown in medium containing 10% FBS, and TEAD reporter activity was analyzed. (D) CCM1 was RNAi-suppressed in LNCaP cells, and the expression levels of CCM1 and representative YAP target genes were analyzed via qPCR. (E) The representative degree of CCM1 suppression in LNCaP, C4-2, and CWR22r cells. The mean  $\pm$  SEM is presented as a ratio to that in each scramble (Scr) control, and graphs were generated from more than three independent experiments. Average levels of CCM1 knockdown were measured from qPCR analysis and presented below each panel. t-test results. Uncropped Blots of Figure 3E can be found in Supplementary File 2. (\*\*\*\*:  $p < 0.0001$ , \*\*\*:  $p < 0.001$ , \*\*:  $p < 0.01$ , \*:  $p < 0.05$ ).

#### 2.4. DDX5 Is a Functional Downstream Mediator of CCM1 in the Regulation of Metastatic Hallmarks

Because the suppression of CCM1 reduced several metastatic hallmarks, we further investigated cadherin switching following the RNAi-mediated silencing of CCM1 or CCM1-interacting proteins. In our previous unreported proteomics study, we identified DDX5 as a novel CCM1-interacting protein and validated the interaction between CCM1 and DDX5 with a co-immunoprecipitation assay (Figure 4A,B). DDX5, also named p68, is a member of the DEAD box family of RNA helicases that contain nine conserved motifs, including the conserved Asp-Glu-Ala-Asp (DEAD) motif. DDX5 is aberrantly expressed/modified in several types of cancers, suggesting that it plays important roles in cancer development and progression [36–38]. HEG1 is a major CCM1-interacting protein with uncertain functions [39], and CCM1 and HEG1 were also found to interact genetically [40]. As observed for CCM1 suppression, HEG1 suppression downregulated N-cadherin and upregulated E-cadherin expression (Figure 4C). Contrary to the changes in cadherin expression after the suppression of CCM1 or HEG1, suppression of DDX5 clearly upregulated N-cadherin and downregulated E-cadherin expression (Figure 4C). Our data indicate that suppression of CCM1 or HEG1 inhibited cadherin switching, whereas suppression of DDX5 induced cadherin switching. Accordingly, suppression of DDX5 upregulated SLUG (Figure 4D), which was contrary to our finding that suppression of CCM1 led to SLUG downregulation (Figure 2D). Our siRNA based HEG1 or DDX5 knockdown showed more than 90% suppression relative to the scramble control. To identify whether DDX5 is a functional downstream mediator of CCM1, we used a co-RNAi silencing strategy for DDX5 and CCM1. Co-suppression of DDX5 and CCM1 decreased E-cadherin and increased N-cadherin expression similarly as observed for silencing of DDX5 alone, restoring the suppression of CCM1-induced changes in cadherin levels (Figure 4E). Next, we suppressed DDX5 in three independent C4-2 shCCM1 cell lines and confirmed that co-suppression of DDX5 restored the migration and invasion of CCM1-silenced PCa cells (Figure 4F). Our data indicate that DDX5 is a major functional downstream mediator of CCM1 in the regulation of metastatic hallmarks such as the migration and invasion of PCa cells.

Although it is believed that DDX5 is upregulated in several tumors compared with its levels in matched normal tissues [41], our PCTA and independent OncoPrint analyses of two PCa datasets [42,43] revealed the downregulation of DDX5 expression in mCRPCa compared with its expression in primary PCa (Figure S4A,B). To reveal the potential impact of genomic rearrangements in the regulation of CCM1 and DDX5 genes, we explored 968 whole-genome sequences of PCa downloaded from four different cohorts including the Canadian prostate cancer genome network [44–46]. Then, we compared the frequency of structural variations in the vicinity of these genes, including copy number alterations and genomic rearrangements. Although both the CCM1 and DDX5 gene loci (7q21.2 and 17q23.3, respectively) are often amplified in a substantial fraction of PCa tumors (approximately 10% for CCM1 and approximately 5% for DDX5), these rates were not increased in mCRPC tissues (Figure S4C). In addition, we did not find any rearrangement candidates near either gene.

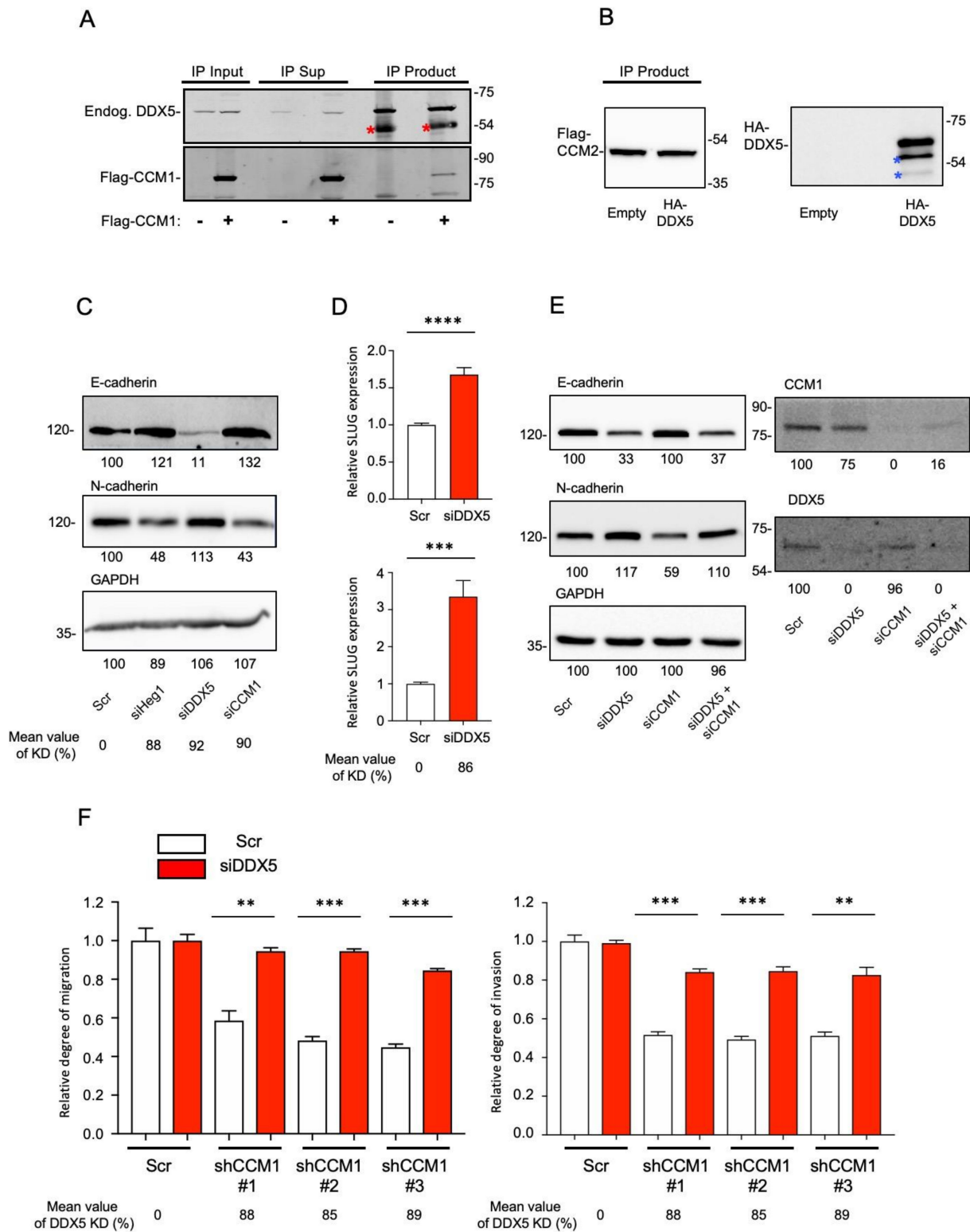


**Figure 4.** DDX5 functions as a mediator of CCM1. (A) Flag-tagged CCM1 was overexpressed in U2OS cells. Endogenous DDX5 were immunoprecipitated with anti-DDX5 antibody from the lysates, and co-immunoprecipitated Flag-CCM1 was immunoblotted with anti-Flag antibody. Uncropped Blots of Figure 4A can be found in Supplementary File 2. (B) HA-tagged DDX5 overexpression plasmid or empty plasmid was transfected into PC3 cells stably overexpressing Flag-tagged WT CCM2. Flag-CCM2 was immunoprecipitated and co-immunoprecipitated HA-tagged DDX5 was immunoblotted with



anti-HA antibody. Red asterisks: heavy chain bands, blue asterisks: degraded products. Uncropped Blots of Figure 4B can be found in Supplementary File 2. (C) Suppression of HEG1, DDX5, and CCM1 using siRNA was performed in PC3 cells, and changes in E-cadherin and N-cadherin expression were analyzed. Band intensities are shown in each panel. Uncropped Blots of Figure 4C can be found in Supplementary File 2. (D) DDX5 was suppressed in PC3 (top) and DU145 (bottom) cells, and SLUG expression was analyzed using qPCR. (E) Individual RNAi silencing of DDX5 or CCM1 and co-silencing of DDX5 and CCM1 were performed in PC3 cells to compare changes in E-cadherin and N-cadherin levels. Band intensities are shown in each panel. Uncropped Blots of Figure 4E can be found in Supplementary File 2. (F) DDX5 expression was suppressed in C4-2 shCCM1 cells, which were plated on Transwell membranes coated without or with Matrigel for migration (left) and invasion assays (right), respectively, incubated for up to 72 h, and stained. The data are presented as the mean  $\pm$  SEM of a ratio to that in intact scramble (Scr) control cells. Functional assays of Figure 4F can be found in Supplementary File 2. Representative images were presented from three independent experiments, and graphs were generated from three independent experiments. Average levels of CCM1 knockdown were measured from qPCR analysis and presented below each panel. t-test results (\*\*\*\*:  $p < 0.0001$ , \*\*\*:  $p < 0.001$ , \*\*:  $p < 0.01$ ).

### 2.5. DDX5 Suppresses YAP/TAZ Signaling

To investigate whether DDX5 regulates YAP/TAZ signaling, we suppressed DDX5 in multiple types of PCa cells. Contrary to the effects of CCM1 suppression, suppression of DDX5 increased TEAD reporter activity in LNCaP, C4-2, and PC3 AR low and high cells (Figure 5A–C). Our siRNA based DDX5 knockdown showed more than 90% suppression relative to the scrambled control. PC3 AR high cells exhibited higher TEAD reporter activity than PC3 AR low cells (Figure 5C). Accordingly, overexpression of WT DDX5 suppressed TEAD reporter activity in all PCa cell types tested (Figure 5D,E and Figure S5A). Our data indicate that DDX5 can uniformly downregulate YAP/TAZ signaling in multiple types of PCa cells regardless of their androgen responsiveness. It has been reported that the phosphorylation of DDX5 at Y593 is important for EMT in HT29 colon cancer cells [38]. To characterize whether Y593 phosphorylation is required for the DDX5-mediated regulation of YAP/TAZ signaling, we overexpressed WT DDX5 or non-phosphorylatable Y593F DDX5 in LNCaP, C4-2, C4-2B, and CWR22r cells. Overexpression of Y593F DDX5 did not alter YAP/TAZ activation, whereas overexpression of WT DDX5 uniformly suppressed YAP/TAZ activation in multiple PCa cell lines (Figure 5D,E and Figure S5A). Increasing ectopic WT DDX5 levels further suppressed TEAD reporter activity, whereas overexpression of Y593F DDX5 had no such effect (Figure 5E), indicating that Y593-phosphorylation of DDX5 was required for the downregulation of YAP/TAZ signaling. Accordingly, suppression of DDX5 upregulated and co-suppression of DDX5 and YAP1 downregulated TEAD reporter activity to a similar level as that of the suppression of YAP1 alone, respectively (Figure 5F and Figure S5B). It is known that YAP1 suppression does not completely abolish TEAD reporter activity based on the presence of residual TAZ expression, which we also validated (Figure S5C). Accordingly, our co-IP experiments using PC3 nuclear lysates revealed that the nuclear YAP-TEAD interaction was increased upon DDX5 suppression (Figure 5G and Figure S5D).

DEAD box RNA helicases use RNA as a substrate to stimulate ATPase activity, and the energy is then used to displace duplex RNA or proteins that bind the RNA substrate [47]. Overexpression of helicase-dead K144N mutant DDX5 also decreased TEAD reporter activity with similar efficiency as WT DDX5, indicating that the RNA helicase activity of DDX5 was not involved in the regulation of YAP/TAZ signaling (Figure 5H). Additionally, with qPCR analysis, we observed that overexpression of Y593 DDX5 increased the expression levels of several representative YAP/TAZ signaling target genes (Figure S5E). We also investigated changes in major mechanisms regulating YAP/TAZ signaling such as alterations in the expression or subcellular localization of YAP or TAZ following DDX5 or CCM1 suppression. The expression level of TAZ was not changed with CCM1 suppression (Figure S5F). Both expression level and subcellular localization of YAP1 were not changed by CCM1 suppression (Figure S5G,H). The subcellular localization of YAP1 was not changed upon DDX5 suppression (Figure S5I). Although our finding that DDX5 interacts with TEAD1 suggests DDX5 as a novel co-repressor of YAP/TAZ signaling, Y593

phosphorylation of DDX5 did not alter the strength of this interaction (Figure S5J). Overexpression of WT or Y593F DDX5 did not change the expression level of total YAP1 (Figure S5K) or the subcellular localization of total YAP1 and S127-phosphorylated cytosolic YAP1 (Figure S5L).

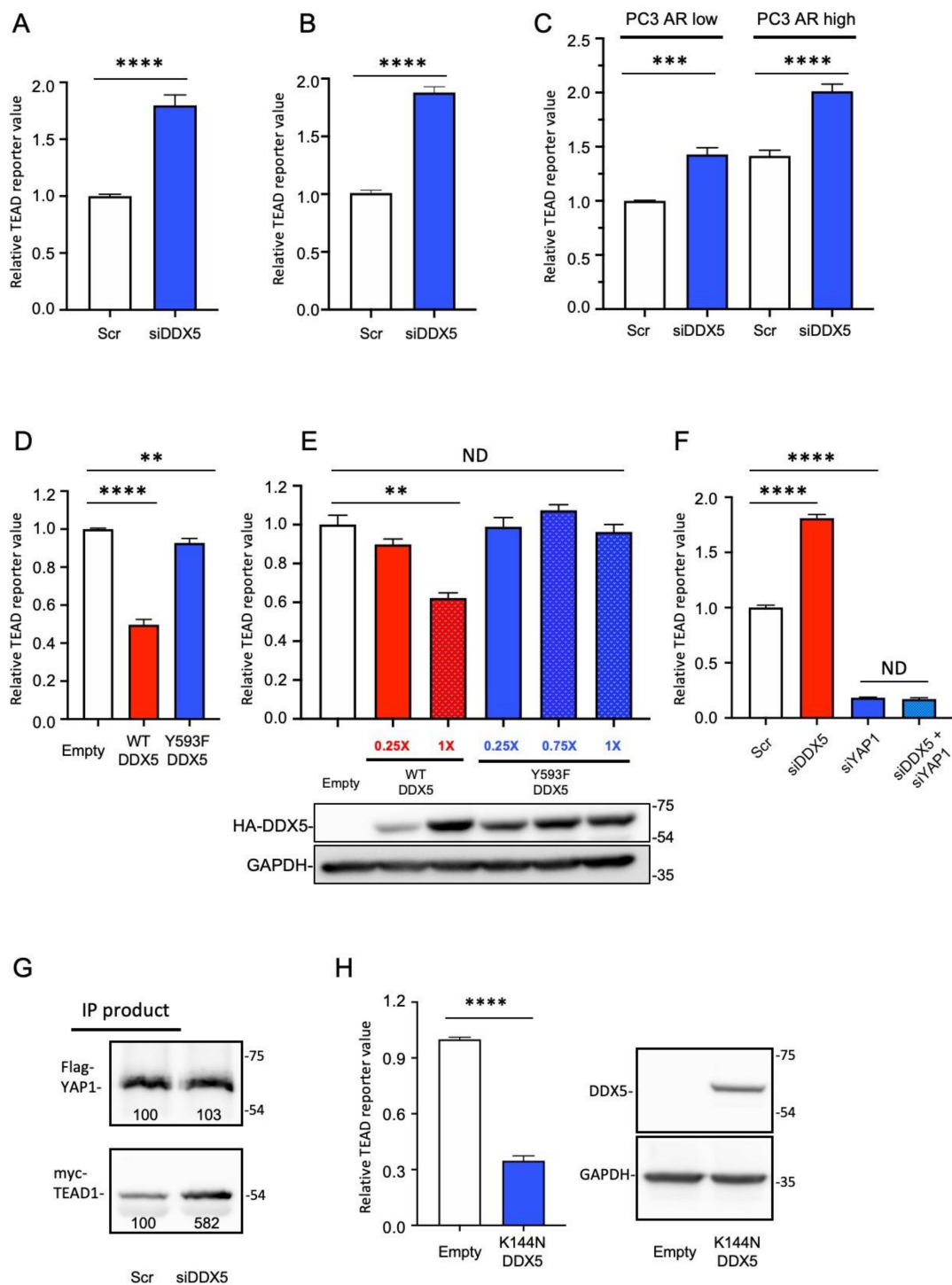


**Figure 5.** DDX5 suppresses YAP/TAZ signaling in prostate cancer cells. DDX5 was RNAi-suppressed in (A) LNCaP, (B) C4-2, and (C) PC3 cells with low or high androgen receptor (AR) expression, grown in regular medium, and TEAD reporter activities were analyzed. (D) WT DDX5 or Y593F DDX5 was overexpressed in C4-2 cells, and lysate was analyzed using the TEAD reporter assay. (E) HA-tagged WT or Y593F DDX5 was overexpressed in C4-2B cells, and each lysate was analyzed using the TEAD reporter assay. Red and blue numbers indicate ratio of DDX5 plasmids transfected. The representative expression levels of overexpressed DDX5 (HA-DDX5) are shown below the graph. Uncropped Blots of Figure 5E can be

found in Supplementary File 2. (F) RNAi suppression of DDX5 or YAP1 alone or co-suppression of DDX5 and YAP1 was performed, and TEAD reporter activity was analyzed in LNCaP cells grown in charcoal-stripped FBS and stimulated with DHT for 18 h. (G) Flag-tagged YAP1 was immunoprecipitated from the nuclear lysates of PC3 cells co-transfected with Flag-tagged YAP, Myc-TEAD1 overexpression plasmids, and siDDX5. The resultant immunoprecipitation products were immunoblotted with anti-Flag and anti-Myc antibodies to detect YAP1 and TEAD1, respectively. Band intensities are shown in each panel. Uncropped Blots of Figure 5G can be found in Supplementary File 2. (H) K114N helicase-dead mutant DDX5 was overexpressed in LNCaP cells, and TEAD reporter activity was analyzed (left). Expression level of the ectopic K114N DDX5 was analyzed with immunoblotting (right). The data in this figure are presented as the mean  $\pm$  SEM relative to that in empty plasmid transfected control or scramble (Scr) control. Graphs were generated from three independent experiments. Empty: empty plasmid transfection. t-test results (\*\*\*\*:  $p < 0.0001$ , \*\*\*:  $p < 0.001$ , \*\*:  $p < 0.01$ , ND: Not significantly different ( $p > 0.05$ )).

As stated previously, YAP/TAZ signaling is a positive regulator of AR signaling, and it is suggested to be responsible for CR in prostate cancer [12,13]. We found that the suppression of DDX5 and YAP1 prominently upregulated and downregulated ARR reporter activity, respectively (Figure S6A). The co-suppression of DDX5 and YAP1 downregulated ARR reporter activity to a similar level as that of the suppression of YAP1 alone. Our data indicate that DDX5 can indirectly upregulate AR signaling via its regulation of YAP/TAZ signaling and that DDX5 regulates AR signaling through YAP rather than TAZ co-activator. Accordingly, we also found that suppression of CCM1 downregulated ARR reporter activity in LNCaP (Figure S6B), CWR22r, C4-2, and C4-2B cells. With qPCR analysis, we also observed that suppression of DDX5 increased the levels of representative AR target genes (Figure S6C). Our data indicate the existence of a functional CCM1-DDX5-YAP-AR signaling pathway in PCa cells.

## 2.6. CCM1 Regulates the Phosphorylation of DDX5 at Y593

As stated, we identified DDX5 as a novel CCM-interacting protein in our previous unreported proteomics study. Moreover, our co-immunoprecipitation (co-IP) assay demonstrated that DDX5 was co-immunoprecipitated with WT CCM1 or CCM2 (Figure 4A,B). As stated, the strong interaction between CCM1 and CCM2 is important for the regulation of CCM signaling in endothelial cells [18,19] and we also validated the interaction in PC3 cells (Figure 6A). Accordingly, we further investigated whether CCM1 is required for the CCM-DDX5 interaction. Compared with the results of WT CCM2 immunoprecipitation, neither immunoprecipitation of L198R CCM2 (CCM1 nonbinding mutant) nor suppression of CCM1 resulted in a notable decrease in the amount of co-immunoprecipitated HA-DDX5 (Figure 6B). Our data indicate that CCM1 was not required for the CCM2-DDX5 interaction.

Because phosphorylation of DDX5 at Y593 was necessary for the suppression of YAP/TAZ signaling and CCM1 and DDX5 had opposite regulatory effects on YAP/TAZ signaling, we hypothesized that CCM1 may downregulate the function of DDX5 by blocking its phosphorylation at Y593. In addition to PDGF, which was previously revealed to induce the phosphorylation of DDX5 at Y593 [38], we serendipitously found in our study that WNT stimulation also induced the phosphorylation at Y593. We used WNT3 and PDGF as positive controls to induce the phosphorylation at Y593. CCM1 was silenced in PC3 cells and non-prostate cancer cell lines (U2OS and HT-29), followed by stimulation with WNT3a (Figure 6C,D) or PDGF ligand (Figure 6D). Notably, suppression of CCM1 further upregulated the basal level of Y593-phosphorylated DDX5 in all cell lines grown in serum-free medium, similarly to what was observed in scramble control cells stimulated with WNT or PDGF (Figure 6C,D), indicating that the CCM1-mediated regulation of Y593 phosphorylation was not limited to PCa cells. As observed for CCM1 suppression, suppression of HEG1 also increased Y593 phosphorylation in DDX5 (Figure 6C). Notably, suppression of HEG1 and CCM1 produced an identical pattern of cadherin switching (Figure 4C).

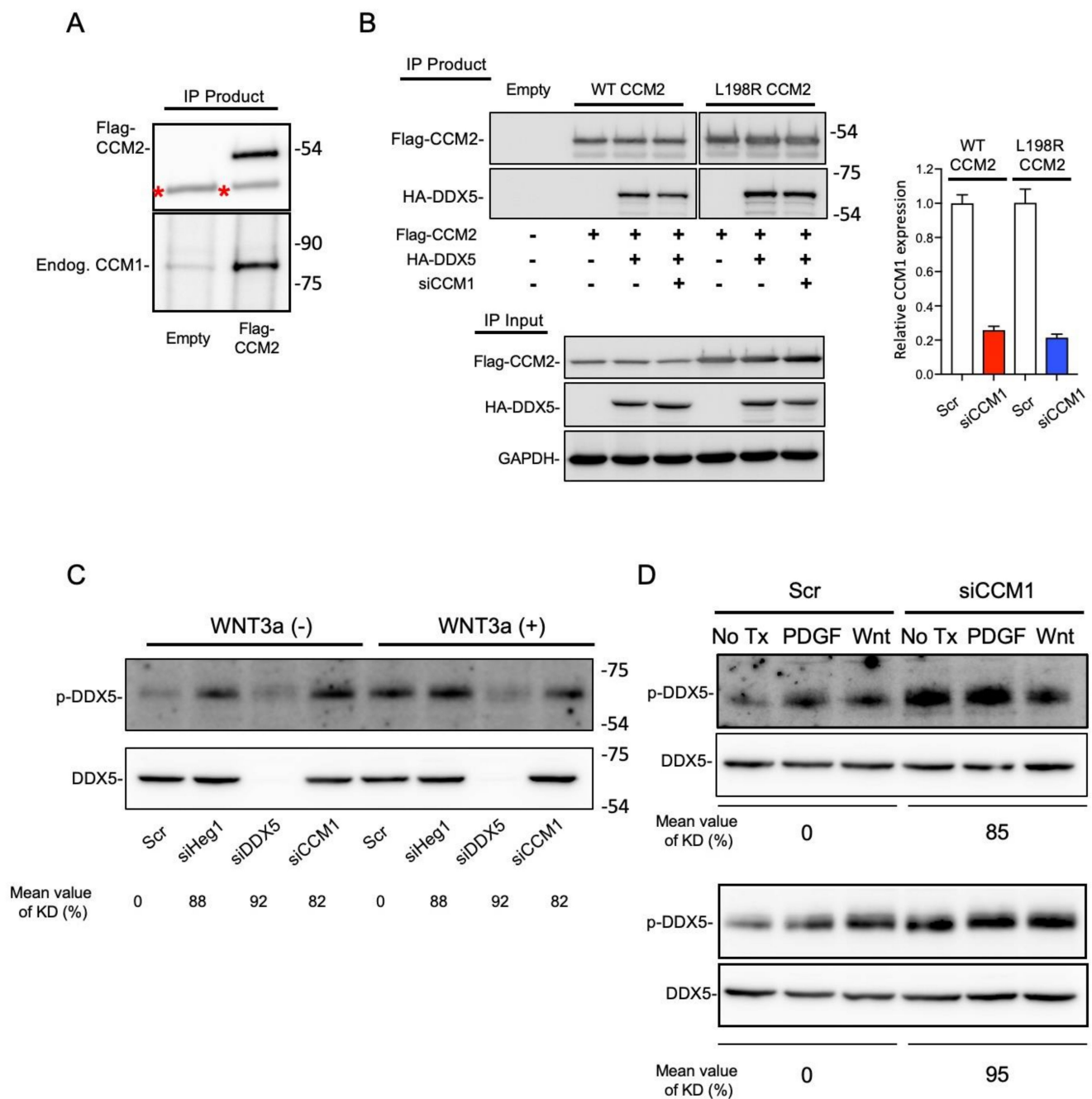


**Figure 6.** CCM1 regulates the phosphorylation of DDX5 at Y593. (A) Flag-tagged CCM2 overexpression plasmid or empty plasmid was transfected into PC3 cells. Flag-CCM2 were immunoprecipitated and co-immunoprecipitated endogenous CCM1 was immunoblotted with anti-CCM1 antibody. Red asterisks: heavy chain bands. Uncropped Blots of Figure 6A can be found in Supplementary File 2. (B) HA-tagged DDX5 overexpression plasmid or empty plasmid was transfected into PC3 cells stably overexpressing Flag-tagged WT CCM2 or L198R CCM2. Additionally, CCM1 was RNAi-silenced in WT or L198R CCM2-expressing cells transfected with HA-DDX5 overexpression plasmids. Flag-CCM2 were immunoprecipitated with anti-Flag antibody, and co-immunoprecipitated DDX5 was immunoblotted with anti-HA antibody (left). Suppression of CCM1 in the same representative experiment was validated with qPCR analysis (right). Uncropped Blots of Figure 6B can be found in Supplementary File 2. (C) PC3 cells were RNAi-silenced as indicated and stimulated with WNT3a. Uncropped Blots of Figure 6C can be found in Supplementary File 2. (D) CCM1 was silenced in U2OS (top) and HT29 (bottom) cells using RNAi, followed by stimulation with WNT3a or PDGF ligand. Uncropped Blots of Figure 6D can be found in Supplementary File 2. Representative images were presented from three independent experiments. Average levels of gene knockdowns were measured from qPCR analysis and presented below each panel. Empty: PC3 cells stably transfected with empty parental plasmid, p-DDX5: Y593-phosphorylated DDX5.

### 3. Discussion

Many recent findings demonstrated that YAP/TAZ and AR signaling serve as the central regulatory mechanisms for prostate tumorigenesis and several cancer-associated pathways can promote YAP/TAZ signaling [14,48]. However, the complete mechanism by which YAP/TAZ signaling becomes hyperactivated and interacts with the stroma, as well as their precise role in PCa development, has not been elucidated. We propose that CCM1 is an important regulator of the YAP/TAZ signaling and AR signaling in PCa cells by releasing YAP/TAZ signaling from DDX5-mediated suppression (Figure 7).

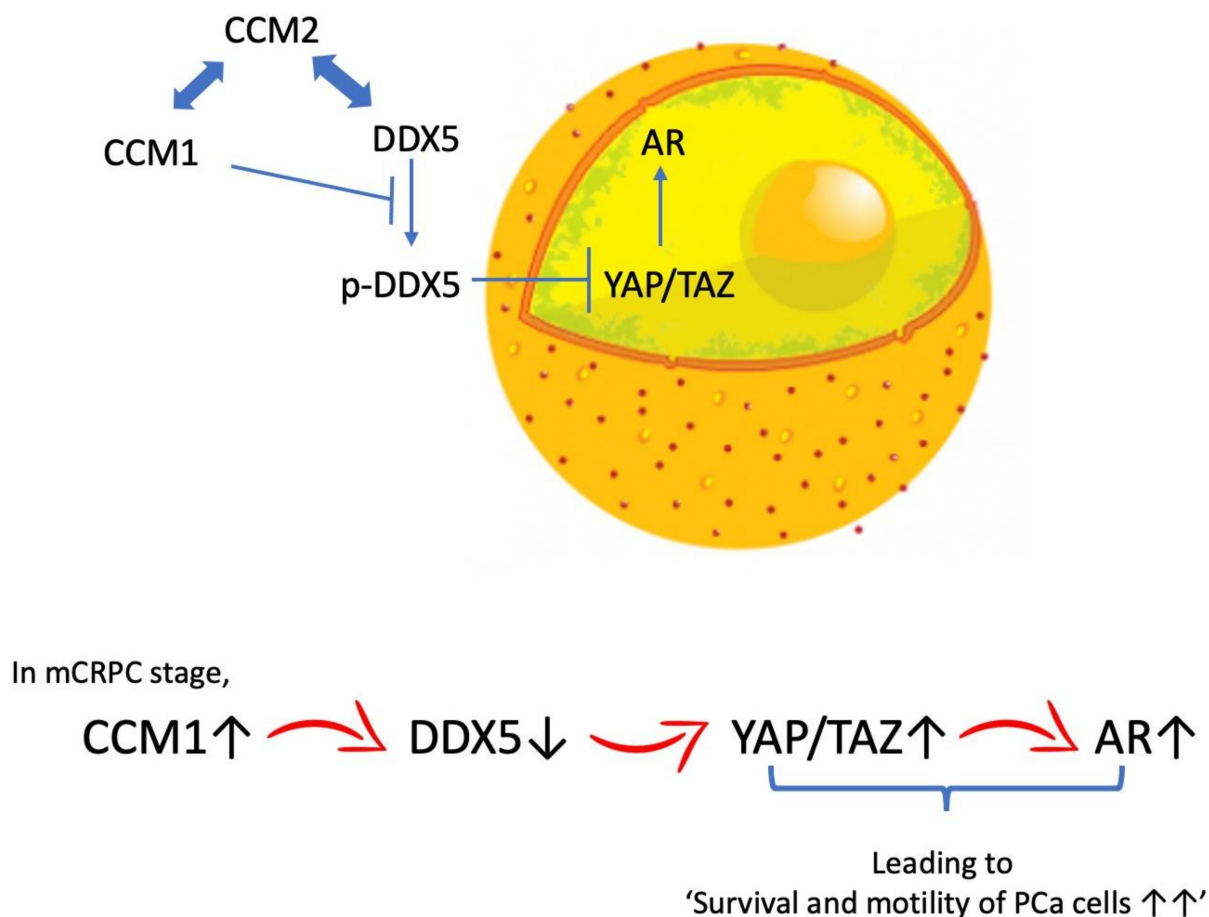


**Figure 7.** Proposed mechanisms of CCM1-mediated regulation of YAP/TAZ and AR signaling. CCM2, a cytosolic protein, is a well-known binding partner of CCM1 and sequesters CCM1 in cytoplasm [18]. Our evidence indicates that CCM1 is important for the suppression of Y593 phosphorylation of DDX5 and that CCM2 may be involved in localization of DDX5 in CCM complexes. We propose that CCM1 is an important regulator of the YAP/TAZ signaling and AR signaling in PCa cells by releasing YAP/TAZ signaling from DDX5-mediated suppression. Each bidirectional arrow indicates an interaction between two proteins.

Our evidence indicates that despite the concomitant activation of multiple pro-tumoral signaling pathways, suppression of CCM1 ameliorated representative metastatic hallmarks, namely motility, invasion and survival [49], in multiple types of both androgen responsive and androgen non-responsive metastatic PCa cells. CCM1 may not be sufficient to induce tumorigenesis, but it appears to unleash the oncogenic potential of multiple cellular signals, promoting cancer progression including the invasiveness and survival of PCa cells. Suppression of DDX5 or CCM1 changed the expression levels of SLUG and TWIST, but not SNAIL, although all three are generally considered important transcription factors involved in EMT in cancer cells. It was demonstrated that the negative feedback between SLUG and SNAIL is differentially regulated in highly and minimally invasive cancer cells [33]. In



breast cancer, SNAIL is involved in early EMT, and decreased SNAIL and increased SLUG expression upregulate phospholipase 2, which is correlated with the increased invasiveness in cancer cells. This may explain why SLUG, but not SNAIL, was notably affected in highly metastatic PCa cells.

Based on genetic aberrations of AR or the increased synthesis of androgens (in the tumor microenvironment [TME]) or adrenal androgen precursors, it has been reported that AR expression is increased [50] and that AR signaling is consistent with the castration level of androgens in patients with mCRPC. However, whether AR signaling is physiologically or supra-physiologically potentiated in the TME of patients with mCRPC is an important open question [51,52]. Our data suggest that elevated levels of CCM1 can potentiate both ligand-dependent and ligand-independent AR signaling in the TME through the upregulation of YAP/TAZ signaling and that the resultant increase in AR signaling may also be important for progression to advanced prostate cancer. Approximately 15–25% of patients with CRPC do not respond to first-line treatment with the “supra-castration” agents abiraterone and enzalutamide [53], and it would be interesting to investigate whether CCM1 is responsible for the non-responsiveness.

Because of the multifocal and heterogeneous nature of human PCa, in which distinct molecular and genetic alterations are associated with various “clones,” the unique and prominent increase of CCM1 expression only in mCRPC was an unexpected finding. Several previous studies investigated genomic alterations in primary PCa and mCRPC and revealed important oncogenic changes responsible for the progression of PCa [3,54]. However, until recently, few large-scale sequencing studies of men with metastatic lethal PCa have been conducted [55]. In the era of PSA screening, most PCa lesions are well differentiated and clinically localized at diagnosis with extremely few lethal events, and these cohorts largely consist of cases that are understood to be de-enriched in men carrying significant genetic risk factors for aggressive disease. In addition, the identification of various somatic mutations responsible for treatment resistance, including CR, from genomic studies of gene mutations and chromosomal DNA arrangements alone without transcriptomic data from heavily treated cancer samples may not reveal selective and crucial alterations in cellular signaling events. These facts may explain why CCM1 has not been previously identified in PCa biology. As the scope of large-scale genomic and transcriptomic analysis of metastatic cancers is mostly confined to heavily treated mCRPC [56], we were unable to differentiate non-treated pure metastatic events from the pool of all metastatic events in heavily treated CRPCs in our PCTA data. Therefore, whether ADT is responsible for the induction of CCM1 and whether the CCM1-mediated upregulation of AR signaling is responsible for CR, in addition to uncontrollable metastasis in patients, will remain outstanding questions for further research.

Our data indicate that DDX5 downregulated YAP/TAZ signaling by suppressing the YAP-TEAD interaction, suggesting that DDX5 may also regulate other nuclear events such as the recruitment of YAP-associated activators or repressors to their target gene promoters. Although DDX5 is known to promote proliferation and tumorigenesis in other cancers, DDX5 downregulation also activates a pro-survival pathway involving mTOR and MDM2 signaling, leading to the inhibition of pro-apoptotic activity in HeLa cells [57], revealing the pleiotropic function of DDX5 depending on the cellular context. For example, phosphorylation of DDX5 at Y593 induced by c-Abl was reported to induce EMT in colon cancer cells [38].

It is believed that DDX5 expression is upregulated in multiple cancer types. Contrarily, we observed that DDX5 expression was downregulated in metastatic PCa compared with that in primary PCa, although we found no evidence of genomic rearrangement. These findings, at least in part, indicate that the previously reported function of DDX5 in other cancer models may not be directly applicable to the biology of PCa. Of note, our functional analysis consistently revealed that DDX5 was a downstream mediator of CCM1 and that DDX5 suppressed a metastatic hallmark in multiple types of PCa cells, adding another layer of complexity to understanding the function of DDX5. Of note, considering the

suppressive effects of DDX5 on YAP/TAZ signaling, downregulation of DDX5 expression in patients with mCRPC appears to further potentiate the CCM1-mediated upregulation of YAP/TAZ signaling and metastasis. In addition to DDX5, we also attempted to identify the cause of CCM1 induction but found that gene rearrangement was not responsible. Therefore, our data indicate that other molecular mechanisms, such as epigenetic changes or cues from the TME, may upregulate CCM1 in metastatic tissues.

Importantly, the incidence of PCa metastasis has dramatically increased because of advancements in therapeutic strategies for patients, indicating the importance of preventing these detrimental metastatic events. We uncovered an interesting scenario in which PCa cells arising in disparate genetic backgrounds appear to share common central molecular events regarding cancer progression.

## 4. Materials and Methods

### 4.1. Cell Culture and Reagents

Human DU145, PC3, LNCaP, C4-2, and CWR22r cells were grown in RPMI medium (Welgene, Gyeongsan, Korea) supplemented with 10% FBS (Welgene, Gyeongsan, Korea) and 1% penicillin/streptomycin (Invitrogen, Carlsbad, CA, USA) at a temperature of 37 °C in an atmosphere of 5% CO<sub>2</sub>. To induce androgen deprivation, RPMI medium supplemented with 10% charcoal-stripped FBS (Scipak Lifesciences, Sacramento, CA, USA) was used. We used Ambion™ Silencer™ Select Validated siRNAs (Ambion, Austin, TX, USA) for transient gene silencing of CCM1 and DDX5.

### 4.2. Generation of Stable Cell Lines

To generate lentiviruses for silencing CCM1, Lenti293 packing cells were plated at  $6 \times 10^5$  cells/well in six-well tissue culture plates and transfected with pLKO.1-puro lentiviral empty vector or shCCM1 vector (Sigma, St.Louis, MO, USA) using X-treme GENE HP DNA transfection Reagent (Roche, Basel, Switzerland). Transfected 293 cells were grown in DMEM containing 30% FBS for 24 h or 48 h. The conditioned medium containing lentiviruses was collected and pooled. Hexadimethrine bromide (Sigma, St.Louis, MO, USA) was added at a final concentration of 8 µg/mL in cell culture medium, and infection was performed by adding lentiviral conditioned medium to PCa cells overnight. Starting the following day, cells were treated with puromycin for 7 days to select lentivirus-infected cells.

### 4.3. Immunoblotting Assay

Cells with stably CCM depletion (shCCM1 cells) via lentiviral shRNA particle transfection were grown to 80% confluence in six-well or 100-mm culture plates. Then, the cells were lysed in RIPA buffer (50 mM Tris-HCl [pH 7.4], 150 mM NaCl, 1% NP-40, 1 mM EDTA, 1 mM EGTA, 2 mM Na<sub>3</sub>VO<sub>4</sub>, 2 mM NaF, 0.25% sodium deoxycholate) containing a cocktail of protease inhibitors (Roche, Basel, Switzerland). The total protein level was quantified using a BCA protein assay kit (Thermo Fisher Scientific, Waltham, MA, USA) according to the manufacturer's protocol. In total, 30–40 µg of total protein were loading into each well of a 10% SDS-PAGE gel and separated using an electroporation system (Bio-Rad, Hercules, CA, USA). Proteins were transferred onto an NC membrane (Whatman, Maidstone, UK), which was cut into strips and blocked for 1 h with 5% skim milk in Tris-buffered saline containing Tween-20 (TTBS) at room temperature. The membranes were later incubated with primary antibody against CCM1 (Abcam, Cambridge, UK), N-cadherin (BD Biosciences, San Jose, CA, USA), E-cadherin (Santa Cruz, Dallas, TX, USA), DDX5 (Abcam, Cambridge, UK), and GAPDH (Protein Tech, Rosemont, IL, USA) in 5% BSA-TTBS overnight at 4 °C and then HRP-conjugated goat anti-rabbit IgG (Jackson, Bar Harbor, ME, USA) or goat anti-mouse IgG (Sigma, St.Louis, MO, USA) secondary antibodies for 1 h at room temperature. The blots were developed using ECL detection reagent (ATTO, Motoasakusa, Japan) and images were taken with an ImageQuant LAS 4000 system (Fujifilm, Minato, Japan).

#### 4.4. Real-Time PCR (qPCR) Analysis

Total RNA from cells was extracted using TRIzol reagent (Takara, Madison, WI, USA), and RNA levels were quantified using spectrophotometry. For each reaction, 1 µg of total RNA served as a template for cDNA synthesis with a PrimeScript™ 1st strand cDNA Synthesis Kit (Takara, Madison, WI, USA). GAPDH and 18S ribosomal RNA were amplified as reference genes for target mRNA. STBR® Primix EX Taq™ II (Takara, Madison, WI, USA) was employed for qPCR analysis.

#### 4.5. Wound-Healing Assay

For monolayer wound-healing assays, cells were plated to confluence in 12-well tissue culture plates. Cell layers were scratched with a 200-µL pipette tip and gently washed with PBS twice, and culture medium was gently added to not perturb the cell monolayer. Migration of cells across the wound edge was observed and photographed at 24 h after wounding.

#### 4.6. Transwell Invasion and Migration Assay

Cell invasion and migration were analyzed using 24-well plate format transfer chambers (SPL) with 8-µm sized pores, and we used Matrigel (Corning, New York, NY, USA) to coat membranes in the transfer chambers for invasion assays. Cells ( $5 \times 10^5$  cells/well) were seeded in each transfer chamber. Medium containing 2% FBS was added to each well of a 24-well plate. The Matrigel invasion chambers were transferred to wells containing the chemoattractant using sterile forceps. A suspension of cells in serum-free medium was loaded into the chambers. Cells were incubated for 24–72 h. The invading cells were fixed with 10% formalin for 15 min at room temperature and stained with hematoxylin for 30 min, and the non-invading cells were removed via scrubbing with a cotton tipped swab. The inserts were washed, and the membrane was photographed using a microscope at  $\times 20$  magnification.

#### 4.7. Soft Agar Assay

To assess colony formation, the CytoSelect 96-Well Cell Transformation assay (Cell Biolabs, San Diego, CA, USA) was used according to the manufacturer's instruction. Briefly, PCa cells were seeded in soft agar at 2500 cells/well. After 7 days of incubation at 37 °C in 5% CO<sub>2</sub>, colony formation was quantified by solubilizing soft agar, lysing cells, and incubating cell lysates with the CyQUANT GR Dye (Cell Biolabs, San Diego, CA, USA) followed by analysis.

#### 4.8. Hanging Drop Culture

Cells were counted using an EVE automated cell counter (Cambridge Bioscience, Cambridge, UK), and the cell count was adjusted to  $1 \times 10^6$  cells/mL. Then, 5 mL of PBS were added to the bottom of the dish to preserve humidity for cell culture. A 20-µL pipette was used to deposit 20-µL drops onto the bottom of the lid. The tissue culture plate lid was inverted, placed in the PBS-filled bottom chamber, and incubated at 37 °C and 5% CO<sub>2</sub>. Hanging drops were monitored daily for 3 days. After 3 days, each drop was pooled and transferred to a small 1.5-mL tube. Centrifugation was performed at  $1200 \times g$  for 3 min at 4 °C, and the resulting pellet was extracted using a RIPA buffer for further studies.

#### 4.9. Immunoprecipitation

Transfected cells were allowed to reach a concentration of 1 µg/µL, and 100 µL was left as the input. In total, 40 µL of Protein G-agarose bead suspension (Santa Cruz, Dallas, TX, USA) was added to 500 µg of lysates and incubated for 1.5 h at 4 °C. After centrifugation, the supernatant was transferred to the new tube. One microgram of the primary antibody was added to the cleared lysates, which were inverted and incubated for 1 h at 4 °C. Protein G-agarose beads were added to the lysates, which were inverted and incubated overnight

at 4 °C. Beads were washed three times with RIPA buffer at 4 °C before bound proteins were eluted with 2× SDS sample buffer and loaded onto SDS-PAGE gels.

#### 4.10. Reporter Assay

In total,  $8 \times 10^4$  cells were plated in each well of a six-well tissue culture plate 16 h before transfection, which was performed using X-treme GENE HP DNA transfection Reagent (Roche) with specific reporter plasmids. A  $\beta$ -galactosidase plasmid was co-transfected to normalize transfection efficiency. After 7 h, the cells were transferred to a new six-well tissue culture plate and incubated for 2 days with medium containing 10% FBS. Subsequently, the cells were washed with PBS and lysed with 200  $\mu$ L of reporter lysis buffer. Then, luciferase reporter activities were assayed as relative light units using a luminometer. The experiments were performed in triplicate, and the results were reported as the mean  $\pm$  SEM. To analyze YAP/TAZ activation, a TEAD reporter (8XGTIIC-luciferase) plasmid was used (Addgene, Watertown, NY, USA). For AR signaling, an ARR2-TK reporter plasmid was kindly provided by Robert Matusik.

#### 4.11. Clonogenic Cell Survival Assay

Cells from a stock culture were plated following the plating of PC3 or DU145 cells into six-well cell culture plates at 1000 cells/well. After 10 days of incubation at 37 °C in 5% CO<sub>2</sub>, medium was removed, and cells were washed with PBS twice. Fixation and staining of colonies were performed using 0.4% crystal violet for 30 min. After removing the staining solution, cells were washed with water twice and dried at room temperature.

#### 4.12. Proliferation Assay and Cell Cycle Analysis

In each well of a 96-well tissue culture plate,  $1 \times 10^4$  cells were plated and incubated with 10  $\mu$ L of Ez-Cytox reagents (DoGen Bio, Seoul, Korea) for 3 hrs. Ez-Cytox assay uses water soluble tetrazolium salt (WST) and measurements were done according to the manufacturer's protocol. For cell cycle analysis, we used an FACS Calibur flow cytometer (Becton, Dickinson and Company, Franklin Lakes, NJ, USA) to analyze cellular DNA stained with propidium iodide.

#### 4.13. Molecular Cohort Analysis

Our PCTA includes more than 4600 clinical PCa specimens. Based on an extensive survey of public resources, we collected 50 PCa datasets from three public databases: Gene Expression Omnibus (<http://www.ncbi.nlm.nih.gov/geo>), ArrayExpress (<http://www.ebi.ac.uk/arrayexpress>), and the UCSC Cancer Genomics Browser (<https://genome-cancer.ucsc.edu>). This collection contains datasets of expression profiles of benign prostate tissue, primary tumors, and metastatic or CRPC.

To assess the association of CCM1 gene expression with overall survival (OS) or metastasis-free survival, clinical information was extracted from the Swedish Watchful Waiting Cohort and Johns Hopkins Cohort. Patients in each cohort were subdivided into categories of "low" (<50th percentile) or "high" ( $\geq$ 50th percentile) CCM1 expression. Kaplan–Meier curves for OS and metastasis-free survival were drawn for each category, and Cox proportional hazard regression analysis was performed for the statistical comparison of survival rates between low and high CCM1 expression groups.

We examined the presence of copy number alterations and genomic rearrangements in the vicinity of the CCM1 and DDX5 genes based on the processed variant calls from the previous studies including the Canadian prostate cancer genome network [44–46]. We quantified the amplification events of these genes by enumerating the number of samples that have copy number gain of the genomic segments containing CCM1 or DDX5 genes. In addition, we investigated genomic rearrangements that might affect the expression level of these genes in the genomic region, including 1 Mb on both sides of the respective genes.

## 5. Conclusions

We report an interesting scenario in which PCa cells arising from disparate genetic backgrounds share CCM1-mediated molecular events that promote cancer progression. Our data indicate that CCM1 upregulated YAP/TAZ signaling and AR signaling by releasing YAP/TAZ signaling from DDX5-mediated suppression via two successive processes, namely the first negative regulation of DDX5 by CCM1 and the second negative regulation of YAP/TAZ signaling by DDX5. CCM1 bears tremendous potential for molecular oncology, and we await future discoveries regarding its function, regulation, and potential diagnostic and therapeutic manipulations at the bedside.

**Supplementary Materials:** The following are available online at <https://www.mdpi.com/2072-6694/13/5/1125/s1>, Supplementary File 1: Figure S1: Expression analysis of CCM1, CCM2, and CCM3, Figure S2: Suppression of CCM1 represses a metastatic hallmark in prostate cancer cells *in vitro*, Figure S3: CCM1-mediated regulation of YAP/TAZ signaling, Figure S4: Expression analysis of DDX5, Figure S5: DDX5 regulates YAP/TAZ signaling, Figure S6: Regulatory mechanisms of DDX5 and CCM1 in AR signaling, Table S1: List of qPCR primers used in this study. Supplementary File 2: Functional assays and uncropped blots.

**Author Contributions:** Conceptualization, J.K. (Jaehong Kim); methodology, S.P. and H.-Y.L.; software, S.R. and H.P.; validation, S.P., H.-Y.L. and H.P.; formal analysis, S.R., Y.S.J. and J.K. (Jayoung Kim); data curation, J.K. (Jayoung Kim); writing—original draft preparation, S.P. and J.K. (Jaehong Kim); writing—review and editing, Y.S.J., E.-G.K., and J.K. (Jayoung Kim); visualization, S.P., H.-Y.L., and J.K. (Jaehong Kim); supervision, J.K. (Jaehong Kim); project administration, J.K. (Jaehong Kim); funding acquisition, J.K. (Jaehong Kim). All authors have read and agreed to the published version of the manuscript.

**Funding:** This work was supported by the Basic Science Research Program, through the National Research Foundation of Korea (NRF), funded by the Ministry of Science, ICT & Future Planning (NRF-2017R1D1A1B03029063 and 2020R1F1A1071980).

**Institutional Review Board Statement:** Not applicable.

**Informed Consent Statement:** Not applicable.

**Data Availability Statement:** Data available on reasonable request.

**Acknowledgments:** We thank Mark H. Ginsberg and Hyun Woo Park for carefully reading and providing helpful comments on this manuscript.

**Conflicts of Interest:** The authors declare no conflict of interest.

## References

1. Spratt, D.E.; Zumsteg, Z.S.; Feng, F.Y.; Tomlins, S.A. Translational and clinical implications of the genetic landscape of prostate cancer. *Nat. Rev. Clin. Oncol.* **2016**, *13*, 597–610. [[CrossRef](#)] [[PubMed](#)]
2. Wyatt, A.W.; Gleave, M.E. Targeting the adaptive molecular landscape of castration-resistant prostate cancer. *EMBO Mol. Med.* **2015**, *7*, 878–894. [[CrossRef](#)] [[PubMed](#)]
3. Barbieri, C.E.; Bangma, C.H.; Bjartell, A.; Catto, J.W.; Culig, Z.; Gronberg, H.; Luo, J.; Visakorpi, T.; Rubin, M.A. The mutational landscape of prostate cancer. *Eur. Urol.* **2013**, *64*, 567–576. [[CrossRef](#)]
4. Jemal, A.; Bray, F.; Center, M.M.; Ferlay, J.; Ward, E.; Forman, D. Global cancer statistics. *Cancer J. Clin.* **2011**, *61*, 69–90. [[CrossRef](#)]
5. Siegel, R.L.; Miller, K.D.; Jemal, A. Cancer statistics, 2018. *Cancer J. Clin.* **2018**, *68*, 7–30. [[CrossRef](#)]
6. Kelly, S.P.; Anderson, W.F.; Rosenberg, P.S.; Cook, M.B. Past, Current, and Future Incidence Rates and Burden of Metastatic Prostate Cancer in the United States. *Eur. Urol. Focus* **2018**, *4*, 121–127. [[CrossRef](#)]
7. Li, J.; Siegel, D.A.; King, J.B. Stage-specific incidence rates and trends of prostate cancer by age, race, and ethnicity, United States, 2004–2014. *Ann. Epidemiol.* **2018**, *28*, 328–330. [[CrossRef](#)]
8. Augello, M.A.; Den, R.B.; Knudsen, K.E. AR function in promoting metastatic prostate cancer. *Cancer Metastasis Rev.* **2014**, *33*, 399–411. [[CrossRef](#)] [[PubMed](#)]
9. Graham, L.; Schweizer, M.T. Targeting persistent androgen receptor signaling in castration-resistant prostate cancer. *Med. Oncol.* **2016**, *33*, 44. [[CrossRef](#)] [[PubMed](#)]
10. Chandrasekar, T.; Yang, J.C.; Gao, A.C.; Evans, C.P. Mechanisms of resistance in castration-resistant prostate cancer (CRPC). *Transl. Androl. Urol.* **2015**, *4*, 365–380. [[CrossRef](#)] [[PubMed](#)]



11. Farooqi, A.A.; Sarkar, F.H. Overview on the complexity of androgen receptor-targeted therapy for prostate cancer. *Cancer Cell Int.* **2015**, *15*, 7. [[CrossRef](#)] [[PubMed](#)]
12. Kuser-Abali, G.; Alptekin, A.; Lewis, M.; Garraway, I.P.; Cinar, B. YAP1 and AR interactions contribute to the switch from androgen-dependent to castration-resistant growth in prostate cancer. *Nat. Commun.* **2015**, *6*, 8126. [[CrossRef](#)] [[PubMed](#)]
13. Zhang, L.; Yang, S.; Chen, X.; Stauffer, S.; Yu, F.; Lele, S.M.; Fu, K.; Datta, K.; Palermo, N.; Chen, Y.; et al. The Hippo Pathway Effector YAP Regulates Motility, Invasion, and Castration-Resistant Growth of Prostate Cancer Cells. *Mol. Cell Biol.* **2015**, *35*, 1350–1362. [[CrossRef](#)]
14. Salem, O.; Hansen, C.G. The Hippo Pathway in Prostate Cancer. *Cells* **2019**, *8*, 370. [[CrossRef](#)] [[PubMed](#)]
15. Cinar, B.; Collak, F.K.; Lopez, D.; Akgul, S.; Mukhopadhyay, N.K.; Kilicarlan, M.; Gioeli, D.G.; Freeman, M.R. MST1 is a multifunctional caspase-independent inhibitor of androgenic signaling. *Cancer Res.* **2011**, *71*, 4303–4313. [[CrossRef](#)]
16. Kim, J. Introduction to cerebral cavernous malformation: A brief review. *BMB Rep.* **2016**, *49*, 255–262. [[CrossRef](#)]
17. Yoruk, B.; Gillers, B.S.; Chi, N.C.; Scott, I.C. Ccm3 functions in a manner distinct from Ccm1 and Ccm2 in a zebrafish model of CCM vascular disease. *Dev. Biol.* **2012**, *362*, 121–131. [[CrossRef](#)] [[PubMed](#)]
18. Zawistowski, J.S.; Stalheim, L.; Uhlik, M.T.; Abell, A.N.; Ancrile, B.B.; Johnson, G.L.; Marchuk, D.A. CCM1 and CCM2 protein interactions in cell signaling: Implications for cerebral cavernous malformations pathogenesis. *Hum. Mol. Genet.* **2005**, *14*, 2521–2531. [[CrossRef](#)]
19. Fisher, O.S.; Liu, W.; Zhang, R.; Stiegler, A.L.; Ghedia, S.; Weber, J.L.; Boggon, T.J. Structural basis for the disruption of the cerebral cavernous malformations 2 (CCM2) interaction with Krev interaction trapped 1 (KRIT1) by disease-associated mutations. *J. Biol. Chem.* **2015**, *290*, 2842–2853. [[CrossRef](#)] [[PubMed](#)]
20. Chan, A.C.; Drakos, S.G.; Ruiz, O.E.; Smith, A.C.; Gibson, C.C.; Ling, J.; Passi, S.F.; Stratman, A.N.; Sacharidou, A.; Revelo, M.P.; et al. Mutations in 2 distinct genetic pathways result in cerebral cavernous malformations in mice. *J. Clin. Invest.* **2011**, *121*, 1871–1881. [[CrossRef](#)] [[PubMed](#)]
21. Song, Y.; Eng, M.; Ghabrial, A.S. Focal defects in single-celled tubes mutant for Cerebral cavernous malformation 3, GCKIII, or NSF2. *Dev. Cell* **2013**, *25*, 507–519. [[CrossRef](#)] [[PubMed](#)]
22. Zhu, Y.; Wu, Q.; Xu, J.F.; Miller, D.; Sandalcioglu, I.E.; Zhang, J.M.; Sure, U. Differential angiogenesis function of CCM2 and CCM3 in cerebral cavernous malformations. *Neurosurg. Focus* **2010**, *29*, E1. [[CrossRef](#)]
23. Glading, A.J.; Ginsberg, M.H. Rap1 and its effector KRIT1/CCM1 regulate beta-catenin signaling. *Dis. Models Mech.* **2010**, *3*, 73–83. [[CrossRef](#)] [[PubMed](#)]
24. Ma, X.; Zhao, H.; Shan, J.; Long, F.; Chen, Y.; Chen, Y.; Zhang, Y.; Han, X.; Ma, D. PDCD10 interacts with Ste20-related kinase MST4 to promote cell growth and transformation via modulation of the ERK pathway. *Mol. Biol. Cell* **2007**, *18*, 1965–1978. [[CrossRef](#)] [[PubMed](#)]
25. Chandran, U.R.; Ma, C.; Dhir, R.; Bisceglia, M.; Lyons-Weiler, M.; Liang, W.; Michalopoulos, G.; Becich, M.; Monzon, F.A. Gene expression profiles of prostate cancer reveal involvement of multiple molecular pathways in the metastatic process. *BMC Cancer* **2007**, *7*, 64. [[CrossRef](#)]
26. You, S.; Knudsen, B.S.; Erho, N.; Alshalalfa, M.; Takhar, M.; Al-Deen Ashab, H.; Davicioni, E.; Karnes, R.J.; Klein, E.A.; Den, R.B.; et al. Integrated Classification of Prostate Cancer Reveals a Novel Luminal Subtype with Poor Outcome. *Cancer Res.* **2016**, *76*, 4948–4958. [[CrossRef](#)] [[PubMed](#)]
27. Sboner, A.; Demichelis, F.; Calza, S.; Pawitan, Y.; Setlur, S.R.; Hoshida, Y.; Perner, S.; Adami, H.O.; Fall, K.; Mucci, L.A.; et al. Molecular sampling of prostate cancer: A dilemma for predicting disease progression. *BMC Med. Genom.* **2010**, *3*, 8. [[CrossRef](#)]
28. Tosoian, J.J.; Trock, B.J.; Landis, P.; Feng, Z.; Epstein, J.I.; Partin, A.W.; Walsh, P.C.; Carter, H.B. Active surveillance program for prostate cancer: An update of the Johns Hopkins experience. *J. Clin. Oncol.* **2011**, *29*, 2185–2190. [[CrossRef](#)]
29. Liu, X.; Chen, X.; Rycaj, K.; Chao, H.P.; Deng, Q.; Jeter, C.; Liu, C.; Honorio, S.; Li, H.; Davis, T.; et al. Systematic dissection of phenotypic, functional, and tumorigenic heterogeneity of human prostate cancer cells. *Oncotarget* **2015**, *6*, 23959–23986. [[CrossRef](#)] [[PubMed](#)]
30. Wheelock, M.J.; Shintani, Y.; Maeda, M.; Fukumoto, Y.; Johnson, K.R. Cadherin switching. *J. Cell Sci.* **2008**, *121*, 727–735. [[CrossRef](#)]
31. Loh, C.Y.; Chai, J.Y.; Tang, T.F.; Wong, W.F.; Sethi, G.; Shanmugam, M.K.; Chong, P.P.; Looi, C.Y. The E-Cadherin and N-Cadherin Switch in Epithelial-to-Mesenchymal Transition: Signaling, Therapeutic Implications, and Challenges. *Cells* **2019**, *8*, 1118. [[CrossRef](#)] [[PubMed](#)]
32. Bussemakers, M.J.; Van Bokhoven, A.; Tomita, K.; Jansen, C.F.; Schalken, J.A. Complex cadherin expression in human prostate cancer cells. *Int. J. Cancer* **2000**, *85*, 446–450. [[CrossRef](#)]
33. Ganesan, R.; Mallets, E.; Gomez-Cambrotero, J. The transcription factors Slug (SNAI2) and Snail (SNAI1) regulate phospholipase D (PLD) promoter in opposite ways towards cancer cell invasion. *Mol. Oncol.* **2016**, *10*, 663–676. [[CrossRef](#)]
34. Hui, L.; Zhang, S.; Dong, X.; Tian, D.; Cui, Z.; Qiu, X. Prognostic significance of twist and N-cadherin expression in NSCLC. *PLoS ONE* **2013**, *8*, e62171. [[CrossRef](#)] [[PubMed](#)]
35. Jividen, K.; Kedzierska, K.Z.; Yang, C.S.; Szlachta, K.; Ratan, A.; Paschal, B.M. Genomic analysis of DNA repair genes and androgen signaling in prostate cancer. *BMC Cancer* **2018**, *18*, 960. [[CrossRef](#)]
36. Dai, T.-Y.; Cao, L.; Yang, Z.-C.; Li, Y.-S.; Tan, L.; Ran, X.-Z.; Shi, C.-M. P68 RNA helicase as a molecular target for cancer therapy. *J. Exp. Clin. Cancer Res.* **2014**, *33*, 64. [[CrossRef](#)]
37. Fuller-Pace, F.V. DEAD box RNA helicase functions in cancer. *RNA Biol.* **2013**, *10*, 121–132. [[CrossRef](#)] [[PubMed](#)]

38. Yang, L.; Lin, C.; Liu, Z.R. P68 RNA helicase mediates PDGF-induced epithelial mesenchymal transition by displacing Axin from beta-catenin. *Cell* **2006**, *127*, 139–155. [[CrossRef](#)] [[PubMed](#)]
39. Gingras, A.R.; Puzon-McLaughlin, W.; Ginsberg, M.H. The structure of the ternary complex of Krev interaction trapped 1 (KRIT1) bound to both the Rap1 GTPase and the heart of glass (HEG1) cytoplasmic tail. *J. Biol. Chem.* **2013**, *288*, 23639–23649. [[CrossRef](#)] [[PubMed](#)]
40. Kleaveland, B.; Zheng, X.; Liu, J.J.; Blum, Y.; Tung, J.J.; Zou, Z.; Sweeney, S.M.; Chen, M.; Guo, L.; Lu, M.M.; et al. Regulation of cardiovascular development and integrity by the heart of glass-cerebral cavernous malformation protein pathway. *Nat. Med.* **2009**, *15*, 169–176. [[CrossRef](#)] [[PubMed](#)]
41. Nyamao, R.M.; Wu, J.; Yu, L.; Xiao, X.; Zhang, F.M. Roles of DDX5 in the tumorigenesis, proliferation, differentiation, metastasis and pathway regulation of human malignancies. *Biochim. Biophys. Acta Rev. Cancer* **2019**, *1871*, 85–98. [[CrossRef](#)] [[PubMed](#)]
42. Grasso, C.S.; Wu, Y.M.; Robinson, D.R.; Cao, X.; Dhanasekaran, S.M.; Khan, A.P.; Quist, M.J.; Jing, X.; Lonigro, R.J.; Brenner, J.C.; et al. The mutational landscape of lethal castration-resistant prostate cancer. *Nature* **2012**, *487*, 239–243. [[CrossRef](#)] [[PubMed](#)]
43. Lapointe, J.; Li, C.; Higgins, J.P.; van de Rijn, M.; Bair, E.; Montgomery, K.; Ferrari, M.; Egevad, L.; Rayford, W.; Bergerheim, U.; et al. Gene expression profiling identifies clinically relevant subtypes of prostate cancer. *Proc. Natl. Acad. Sci. USA* **2004**, *101*, 811–816. [[CrossRef](#)] [[PubMed](#)]
44. Espiritu, S.M.G.; Liu, L.Y.; Rubanova, Y.; Bhandari, V.; Holgersen, E.M.; Szyca, L.M.; Fox, N.S.; Chua, M.L.K.; Yamaguchi, T.N.; Heisler, L.E.; et al. The Evolutionary Landscape of Localized Prostate Cancers Drives Clinical Aggression. *Cell* **2018**, *173*, 1003–1013. [[CrossRef](#)]
45. Fraser, M.; Sabelnykova, V.Y.; Yamaguchi, T.N.; Heisler, L.E.; Livingstone, J.; Huang, V.; Shiah, Y.J.; Yousif, F.; Lin, X.; Masella, A.P.; et al. Genomic hallmarks of localized, non-indolent prostate cancer. *Nature* **2017**, *541*, 359–364. [[CrossRef](#)]
46. Quigley, D.A.; Dang, H.X.; Zhao, S.G.; Lloyd, P.; Aggarwal, R.; Alumkal, J.J.; Foye, A.; Kothari, V.; Perry, M.D.; Bailey, A.M.; et al. Genomic Hallmarks and Structural Variation in Metastatic Prostate Cancer. *Cell* **2018**, *174*, 758–769. [[CrossRef](#)]
47. Wang, H.; Gao, X.; Yang, J.J.; Liu, Z.R. Interaction between p68 RNA helicase and Ca<sup>2+</sup>-calmodulin promotes cell migration and metastasis. *Nat. Commun.* **2013**, *4*, 1354. [[CrossRef](#)] [[PubMed](#)]
48. Collak, F.K.; Demir, U.; Ozkanli, S.; Kurum, E.; Zerk, P.E. Increased expression of YAP1 in prostate cancer correlates with extraprostatic extension. *Cancer Biol. Med.* **2017**, *14*, 405–413. [[CrossRef](#)] [[PubMed](#)]
49. Welch, D.R.; Hurst, D.R. Defining the Hallmarks of Metastasis. *Cancer Res.* **2019**, *79*, 3011–3027. [[CrossRef](#)] [[PubMed](#)]
50. Robinson, D.; Van Allen, E.M.; Wu, Y.M.; Schultz, N.; Lonigro, R.J.; Mosquera, J.M.; Montgomery, B.; Taplin, M.E.; Pritchard, C.C.; Attard, G.; et al. Integrative clinical genomics of advanced prostate cancer. *Cell* **2015**, *161*, 1215–1228. [[CrossRef](#)] [[PubMed](#)]
51. Pakula, H.; Xiang, D.; Li, Z. A Tale of Two Signals: AR and WNT in Development and Tumorigenesis of Prostate and Mammary Gland. *Cancers* **2017**, *9*, 14. [[CrossRef](#)] [[PubMed](#)]
52. Linja, M.J.; Savinainen, K.J.; Saramaki, O.R.; Tammela, T.L.; Vessella, R.L.; Visakorpi, T. Amplification and overexpression of androgen receptor gene in hormone-refractory prostate cancer. *Cancer Res.* **2001**, *61*, 3550–3555. [[PubMed](#)]
53. Antonarakis, E.S. Current understanding of resistance to abiraterone and enzalutamide in advanced prostate cancer. *Clin. Adv. Hematol. Oncol.* **2016**, *14*, 316–319.
54. Baca, S.C.; Prandi, D.; Lawrence, M.S.; Mosquera, J.M.; Romanel, A.; Drier, Y.; Park, K.; Kitabayashi, N.; MacDonald, T.Y.; Ghandi, M.; et al. Punctuated evolution of prostate cancer genomes. *Cell* **2013**, *153*, 666–677. [[CrossRef](#)]
55. Isaacs, W.B.; Xu, J. Current progress and questions in germline genetics of prostate cancer. *Asian J. Urol.* **2019**, *6*, 3–9. [[CrossRef](#)] [[PubMed](#)]
56. Frank, S.; Nelson, P.; Vasioukhin, V. Recent advances in prostate cancer research: Large-scale genomic analyses reveal novel driver mutations and DNA repair defects. *F1000Res.* **2018**, *7*. [[CrossRef](#)] [[PubMed](#)]
57. Kokolo, M.; Bach-Elias, M. Downregulation of p68 RNA Helicase (DDX5) Activates a Survival Pathway Involving mTOR and MDM2 Signals. *Folia Biol.* **2017**, *63*, 52–59.